SAGE-Hindawi Access to Research
Journal of Nucleic Acids
Volume 2010, Article ID 763658, 11 pages
doi:10.4061/2010/763658

Research Article

Structural Properties of G,T-Parallel Duplexes

Anna Aviñó,[1] Elena Cubero,[2] Raimundo Gargallo,[3] Carlos González,[4] Modesto Orozco,[2] and Ramon Eritja[1]

[1] *Institute for Research in Biomedicine, IQAC-CSIC, CIBER-BBN Networking Centre on Bioengineering, Biomaterials and Nanomedicine, Edifici Helix, Baldiri Reixac 15, 08028 Barcelona, Spain*
[2] *Joint IRB-BSC Program on Computational Biology, Institute for Research in Biomedicine and Barcelona Supercomputing Center, Department of Biochemistry, University of Barcelona, Baldiri Reixac 10-12, 08028 Barcelona, Spain*
[3] *Department of Analytical Chemistry, University of Barcelona, Diagonal 647, 08028 Barcelona, Spain*
[4] *Department of Spectroscopy and Molecular Structure, Instituto de Química Física Rocasolano, C.S.I.C. Serrano 119, 28006 Madrid, Spain*

Correspondence should be addressed to Ramon Eritja, recgma@cid.csic.es

Received 19 August 2009; Accepted 15 November 2009

Academic Editor: Luis A. Marky

The structure of G,T-parallel-stranded duplexes of DNA carrying similar amounts of adenine and guanine residues is studied by means of molecular dynamics (MD) simulations and UV- and CD spectroscopies. In addition the impact of the substitution of adenine by 8-aminoadenine and guanine by 8-aminoguanine is analyzed. The presence of 8-aminoadenine and 8-aminoguanine stabilizes the parallel duplex structure. Binding of these oligonucleotides to their target polypyrimidine sequences to form the corresponding G,T-parallel triplex was not observed. Instead, when unmodified parallel-stranded duplexes were mixed with their polypyrimidine target, an interstrand Watson-Crick duplex was formed. As predicted by theoretical calculations parallel-stranded duplexes carrying 8-aminopurines did not bind to their target. The preference for the parallel-duplex over the Watson-Crick antiparallel duplex is attributed to the strong stabilization of the parallel duplex produced by the 8-aminopurines. Theoretical studies show that the isomorphism of the triads is crucial for the stability of the parallel triplex.

1. Introduction

DNA can form a large range of helical structures, including duplexes, triplexes, and tetraplexes [1–4]. The right-handed B-type duplex is the most common structure, but even now, five decades after the discovery of the B-DNA, new helical conformations of DNA are being described. This demonstrates that DNA has great flexibility and polymorphism, depending on sequence, chemical modifications, and alterations in the DNA environment [1].

Most DNA duplexes are antiparallel, but parallel arrangements have been found in both hairpins and linear DNAs [5–9]. Sequences with a propensity to form parallel DNAs have been found in specific chromosome regions [10–12], and they could have an evolutionary role [13]. Moreover, certain types of parallel-stranded DNA can be excellent templates for the formation of triplexes, and so they can be used to develop more powerful antisense oligonucleotides [14, 15]. Parallel DNA may also be used to prepare aptamers that may block proteins similarly to the antiparallel hairpin loops stabilized by combinations of Watson-Crick and non-canonical intramolecular interactions discovered by SELEX [16, 17].

Oligonucleotides able to form triplexes with target nucleic acid sequences have been largely studied as DNA-binding molecules of potential interest in diagnosis or therapeutics [2, 3, 18, 19]. Typically, triplexes are formed in homopurine-homopyrimidine sequences of duplex DNA by interaction with a single-stranded triplex-forming oligonucleotide, which binds to the major groove of Watson-Crick double-helical DNA, parallel or antiparallel to the homopurine strand, via Hoogsteen or reversed-Hoogsteen hydrogen bonding. However, an interesting alternative approach will be to use duplexes (parallel or antiparallel clamps) containing the Hoogsteen or reverse Hoogsteen pairs and targeting a single stranded fragment of DNA or RNA [20–23].

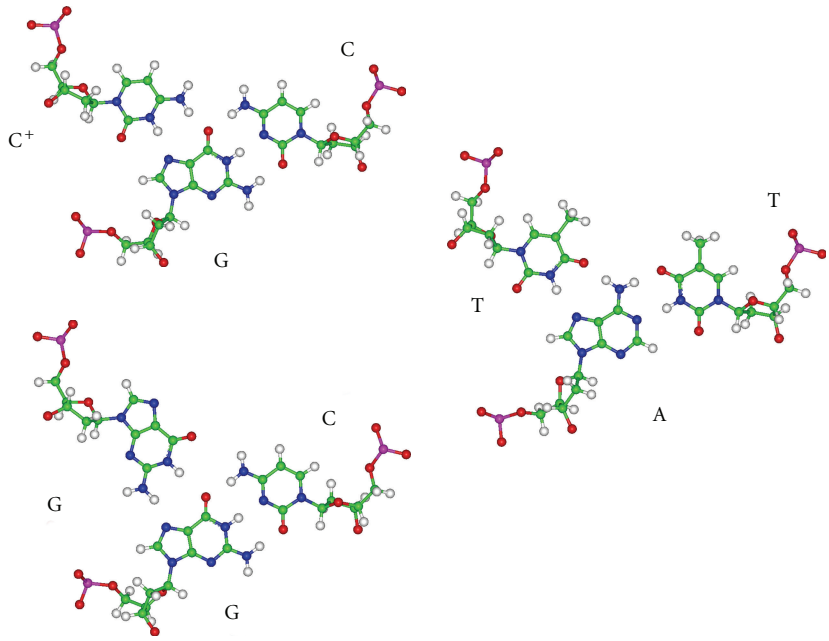

Scheme 1: Hypothetical triads in parallel-G,T and parallel-C,T triplexes.

8-Aminoadenine [20] and 8-aminoguanine [21] stabilize parallel duplexes [22] and triplexes as well as antiparallel triplexes [23]. 8-Aminoadenine may stabilize parallel duplexes and triplexes because the amino group is positioned to form an extra hydrogen bond with the keto group of the Hoogsteen thymidine (Scheme 1). This stabilization has been shown for C,T-parallel duplexes [22] and triplexes [15]. In this study, we have prepared several G,T-duplexes and examined the stability of G,T-parallel duplexes and triplexes formed by using G,T-parallel duplexes carrying 8-aminoadenine and 8-aminoguanine. G,T-Parallel duplexes have been studied [24] but there is little information on G,T-parallel triplexes [25].

In this work, theoretical calculations predict and experiments demonstrate that the presence of 8-aminopurines stabilizes the G,T-parallel duplex but the modified parallel duplex does not bind to its polypyrimidine target. Detailed analysis of the data shows that the isomorphism of the triads is more important than the possible pattern of triple helix hydrogen bonding to define the triplex structure.

2. Materials and Methods

2.1. Chemicals. Phosphoramidites and ancillary reagents used during oligonucleotide synthesis were from Applied Biosystems (PE Biosystems Hispania S.A., Spain), Glen Research Inc. (USA), Transgenomics Ltd. (Scotland), and Link Technologies Ltd. (Scotland). The rest of the chemicals were purchased from Aldrich, Sigma, or Fluka (Sigma-Aldrich Química S.A., Spain).

2.2. Oligonucleotide Synthesis. Oligonucleotide sequences (1–8, Table 1) were prepared on an automatic Applied Biosystems 392 DNA synthesizer on 0.2 μmol (LV200) scale using commercially available chemicals. The phosphoramidite of hexaethyleneglycol and the reversed G and reversed T phosphoramidites were obtained from commercial sources (Glen Research, Transgenomics, Link Technologies). The parallel duplexes were synthesized as follows: First, the polypurine sequence was assembled using standard G and A phosphoramidites. Then, a hexaethyleneglycol linker was added. Finally, The G,T-sequence was assembled using reversed G and T phosphoramidites. After the assembly of the sequences, oligonucleotide-supports were treated with 32% aqueous ammonia at 55°C for 16 h. Ammonia solutions were concentrated to dryness and the products were purified by reversed-phase HPLC as follows: Solvent A: 5% acetonitrile in 100 mM triethylammonium acetate pH 6.5 and solvent B: 70% acetonitrile in 100 mM triethylammonium acetate pH 6.5; Columns: PRP-1 (Hamilton), 250 × 10 mm; Flow rate: 3 ml/min; A 30-minute linear gradient from 10% to 80% B (DMT on) or a 30-minute linear gradient from 0% to 50% B (DMT off). In addition, oligonucleotides used for NMR studies were converted to the sodium salt by passing through a Dowex 50Wx4 (Na^+ form) followed by desalting over a Sephadex G-25 (NAP-10) column eluted with water. Yields are between 10 and 20 $O.D._{260}$ units.

2.3. Melting Experiments by UV Spectroscopy. The optical melting experiments were performed using a Shimadzu UV spectrophotometer equipped with a Peltier heater. Solutions of equimolar amounts of the parallel GT-duplexes or control oligonucleotides with or without the corresponding target pyrimidine strand were mixed in 10 mM sodium cacodylate, 50 mM $MgCl_2$ pH 7.2 (or 2 M NaCl, or 2 M NaCl, 5 mM $ZnCl_2$). The solutions were heated to 90°C and allowed to

Table 1: Sequences of the G,T-parallel clamps, control oligonucleotides, and their targets.

No.	Type	Sequence
1	Parallel clamp	3′-GTTGGTGGTGT-5′-AGAGGAGGAAG-3′
2	Target 1	3′-TCTCCTCCTTC-5′
3	Complementary to 2	5′-AGAGGAGGAAG-3′
4	Parallel clamp	3′-TGTGGTGGTTG-5′-$(EG)_6$-5′-GAAGGAGGAGA-3′
5	Parallel clamp	3′-TGTGGTGGTTG-5′-$(EG)_6$-5′-GAAGGA^NGGA^NGA-3′
6	Parallel clamp	3′-TGTGGTGGTTG-5′-$(EG)_6$-5′-G$A^N A^N$GGA^NGGA^NGA-3′
7	Parallel clamp	3′-TGTGGTGGTTG-5′-$(EG)_6$-5′-GAAG^NAGG^NAGA-3′
8	Target 2	3′-CTTCCTCCTCT-5′
9	Control	3′-GGTTGGTTGGT-5′-$(EG)_6$-5′-GAAGGA^NGGA^NGA-3′
10	Complementary to **8**	5′-GAAGGAGGAGA-3′
11	2′-OMe-RNA target 2	3′-*CUUCCUCCUCU*-5′

A^N = 8-aminoadenine, G^N = 8-aminoguanine, -$(EG)_6$= hexaethyleneglycol, *C*,*U* = 2′-O-methyl-RNA.

cool slowly to room temperature, and samples were then stored in a refrigerator overnight. UV absorption spectra and melting experiments (absorbance versus temperature) were recorded in 1 cm path-length cells using a spectrophotometer, which had a temperature controller with a programmed temperature increase of 0.5°C/min. Denaturation curves were run on a concentration of 5-6 μM at 260 nm. Melting temperatures (T_m) and free energy values (ΔG) were derived by computer-fitting the denaturation data, using the MeltWin program. Thermodynamic data were calculated as the mean of three independent melting experiments. Uncertainty in *Tm* and individual free energy measurements is estimated at ±0.5°C and ±10%, respectively. Free energy values are given at 37°C.

2.4. Circular Dichroism. Samples were prepared as described for the melting experiments by UV spectroscopy. The CD spectra were recorded on a Jasco J-810 spectropolarimeter attached to a Julabo F/25HD circulating water bath in 1 cm path-length quartz cylindrical cells. Spectra were recorded at room temperature using a 50 nm/min scan rate, a spectral band width of 1 nm, and a time constant of 4 seconds. All the spectra were corrected with the buffer blank, normalized to facilitate comparisons, and noise-reduced using Matlab software.

2.5. NMR Experiments. An equimolar mixture of the parallel GT-clamp oligodeoxynucleotide **1** with or without the target Watson-Crick pyrimidine strand **2** was prepared in 300 μL of 9 : 1 H_2O/D_2O, 25 mM sodium phosphate buffer, and 50 mM $MgCl_2$ pH 7. The same buffer conditions were used for parallel duplex **7**. The final oligonucleotide concentration was around 0.4 mM and 0.2 mM for samples **1** and **7**, respectively. Spectra were acquired in a Bruker spectrometer operating at 600 MHz equipped with a cryoprobe, and processed with the X-WINMR software. Water suppression was performed by using a jump-and-return pulse sequence with a null excitation in the water signal. All experiments were performed at 5°C.

2.6. Theoretical Methods. Theoretical simulations using state-of-the-art molecular dynamic techniques were used to gain structural details on the different duplexes/triplexes considered. In a first step, parallel triplex of sequence d(AGAGGAGGAAG)·d(CTTCCTCCTCT)-d($TC^+TC^+C^+TC^+C^+TTC^+$) (ps-Triplex I) was built from manipulation of a poly(GA) parallel triplex previously studied in the group [26, 27]. The structure was neutralized by adding a suitable number of Na^+, solvated by around 5000 water molecules, partially optimized, thermalized (T = 298 K), and equilibrated using our standard multistage protocol for 200 ps [28, 29]. The equilibrated structure was used as starting point for an unrestrained control 10-nanosecond simulation, as well as to generate a starting model for a triplex with sequence: d(AGAGGAGGGAAG)·d(CTTCCTCCTCT)-d(TGTGGTGGTTG) (ps-Triplex II). The equilibrated structure of this new triplex was then subject of 10-nanoseconds of unrestrained MD simulation following conditions noted above. The equilibrated structures of both ps-Triplex I and ps-Triplex II were used to generate standard models of the corresponding parallel duplex (ps-Duplex I and ps-Duplex II) by removal of the Watson-Crick pyrimidine strands. Such models were neutralized, hydrated, minimized, thermalized, and equilibrated as described above. The equilibrated duplexes were used as starting point of 10 nanoseconds of unrestrained MD simulation. An additional control simulation was performed using the same protocol for a Watson-Crick antiparallel duplex (aps-Duplex) with sequence d(AGAGGAGGAAG)·d(CTTCCTCCTCT).

All trajectories were collected at constant pressure (P = 1 atm) and temperature (T = 298 K), with standard AMBER relaxation times. Periodic boundary conditions in conjunction with periodic boundary conditions and the Particle Mesh Ewald method [30] were used to account for long range electrostatic effects. SHAKE [31] was used to constraint all bonds, allowing us to use 2 fs time step for integration of Newton's equations.

As in other previous works thermodynamic integration coupled to MD simulations (MD/TI) [15, 20–23, 32];

Table 2: Melting temperature (*Tm*) and free energies of the parallel duplex-to-random-coil transition.[a]

Parallel clamp	*Tm* (°C)	ΔG (Kcal/mol)
1	51.8	−1.3
4	55.8	−2.0
5	61.7	−2.7
6	62.8	−3.1
7	61.3	−2.4

[a]50 mM $MgCl_2$, 10 mM sodium cacodylate pH 7.2.

was done to evaluate the impact of the adenine → 8-aminoadenine substitution (at the 6th position) on the stability of ps-Duplex II and ps-Triplex II. As described in detail elsewhere [15, 20–23, 32], the A → A^N mutation was repeated 8 times using both "forward" and "reverse" directions with 21 and 41 (20 ps) windows in duplex, triplex, and a model of single strand (d(GGAGG); values were combined using standard thermodynamic cycles to obtain the impact of the mutation in the single → ps Duplex, single → ps-Triplex and ps-Duplex → ps-Triplex folding equilibria. "Reverse" mutations models of the corresponding oligonucleotides with 8-aminoadenine at the 6th position were created and equilibrated for 5 nanoseconds using simulation protocol described above.

The parmbsc0 [33] revision of AMBER force-field for nucleic acids [34, 35] supplemented with previously developed parameters for 8-amino purines [15, 20–23, 32] was used to describe DNA interactions, while TIP3P model was used to represent waters [36]. Trajectories and analysis were done using the AMBER9.0 suite of programs [37] as well as using "in house" developed software.

3. Results and Discussion

3.1. Unmodified Duplexes Bind Their Target to Form Antiparallel Watson-Crick Duplexes. First we studied triplex formation by G,T-duplexes carrying natural bases. To this end a G,T-parallel clamp (**1**, Table 1) designed to bind the 11-base polypyrimidine sequence in the West Nile virus genome (**2**, Table 1) was prepared. The clamp was synthesized as described elsewhere [9–11]. First, the polypurine sequence was assembled using standard G and A phosphoramidites, followed by the addition of the hexaethyleneglycol (= 3, 6, 9, 12, 15-pentaoxaheptadecane-1, 17-diol, $(EG)_6$) linker. Finally, the G,T-sequence was assembled using reversed G and T phosphoramidites.

The parallel duplex-to-random-coil transition of clamp **1** was measured spectrophotometrically at pH 7.2 in the presence of magnesium. A single transition was observed (Figure 1). The UV data were analyzed using a two-state melting model with the Meltwin program (Table 2). Melting temperature (*Tm*) was 51.8°C with a free energy change associated with the transition of −1.3 kcal/mol. This is consistent with previous data on hairpins of this type [24].

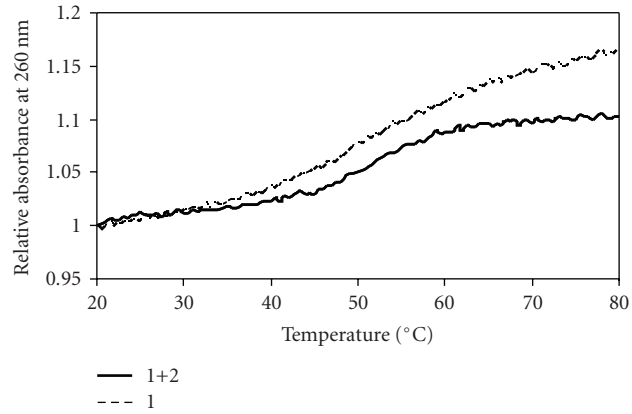

Figure 1: Melting curves of parallel clamp **1** and the complex formed by **1** and its target **2** (Conditions 50 mM $MgCl_2$, 10 mM sodium cacodylate pH 7.2).

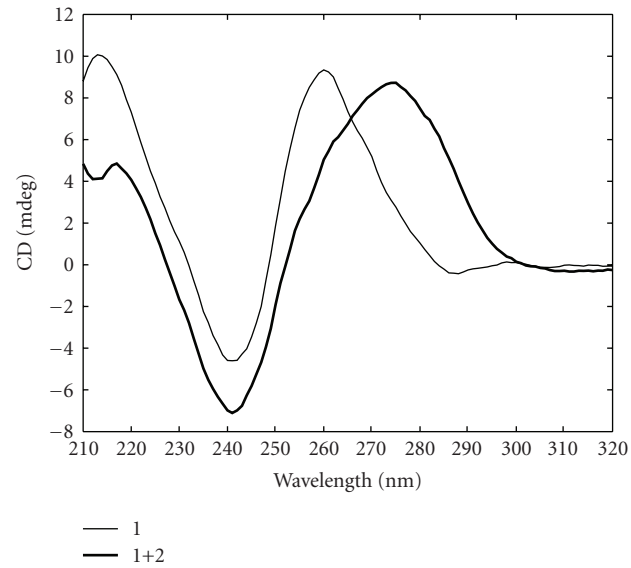

Figure 2: Circular dichroism spectra of parallel clamp **1** and the complex formed by **1** and its target **2** (Conditions 50 mM $MgCl_2$, 10 mM sodium cacodylate pH 7.2).

The circular dichroism (CD) spectrum of clamp 1 (Figure 2) was also consistent with reported spectra of G,T-parallel duplexes [24]. The CD spectrum consisted of a positive maximum at 260 nm, zero-crossover at 252 nm, and a negative band at 241 nm. The NMR spectrum of clamp 1 (Figure 3) consisted of broad signals. This broadening is attributable to the presence of multiple structures in a conformational exchange (conformational heterogeneity). However, the observation of imino signals in the 12–14 ppm region of the exchangeable protons indicates the occurrence of AT base-pairs (Figure 3). The line broadening is even more pronounced at higher temperatures.

The effect of the addition of the polypyrimidine target strand **2** was studied by UV, CD, and NMR. The melting curve of the complex formed by clamp **1** and target **2** gave a more cooperative curve than the clamp alone (Figure 1) but

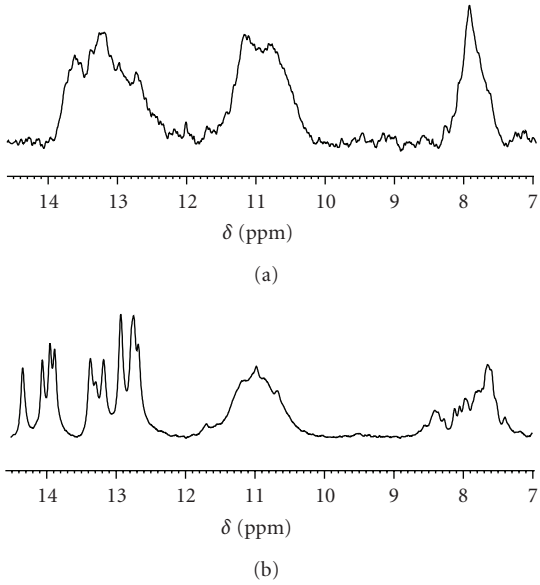

Figure 3: NMR of (a) parallel clamp **1** and (b) the complex formed by **1** and its target **2** (Conditions 50 mM $MgCl_2$, 10 mM sodium phosphate).

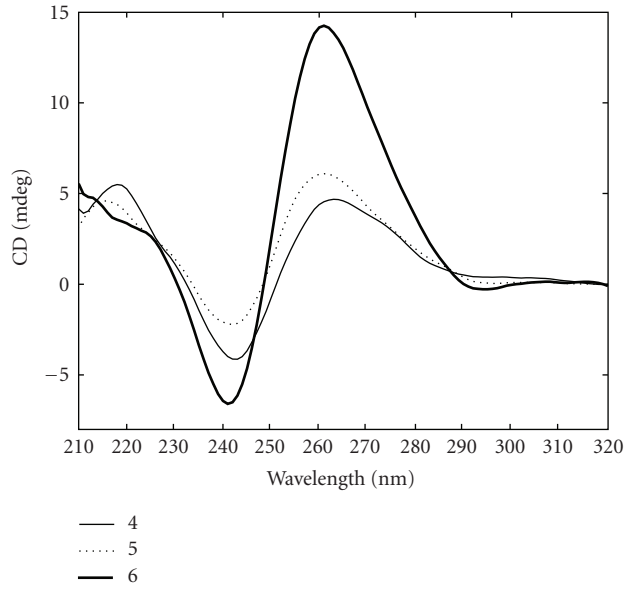

Figure 4: Circular dichroism spectra of parallel clamp **4**, parallel clamp **5,** and parallel clamp **6** (Conditions 50 mM $MgCl_2$, 10 mM sodium cacodylate pH 7.2

the observed *Tm* was similar (*Tm* 51.9°C). The CD and NMR spectra of the complex were different from those of the clamp alone. The negative band at 240 nm of the CD spectrum remained but the positive maximum moved to 277 nm and the zero-crossover moved to 255 nm (Figure 2). The overall CD spectrum of the complex was similar to the spectrum of a B-family duplex.

After the addition of the target strand, the NMR spectra showed some narrow signals between 12 and 14 ppm and a broad band around 11 ppm (Figure 3). The narrow signals correspond with imino protons of T and G involved in Watson-Crick base-pairing. The broad band observed near 11 ppm arises from G's imino protons that may be involved in a G.G basepair or simply unpaired. Taken together, these data indicated that clamp **1** was interacting with target **2,** forming either a duplex with the unpaired G,T-strand or a G,T-parallel triplex. In order to distinguish between these two possibilities we obtained the melting curves and CD spectra in 2 M NaCl and 2 M NaCl, 10 mM $ZnCl_2$. The presence of Zn^{2+} ions stabilizes the G,T-parallel triplex, giving a clear change in the CD spectra [25].

We analyzed the melting curves of the complex formed by the parallel clamp **1** and its polypyrimidine target **2**. These oligonucleotides were designed to form a G,T-parallel triplex. A control duplex was formed by mixing oligonucleotides **3** and **2**. The melting curves of the complex formed by parallel clamp and its target had the same shape as the melting curve of control duplex in all three conditions (50 mM Mg^{2+}, 2 M Na^+ and 2 M Na^+, 10 mM Zn^{2+}). Consequently, the melting temperatures and free energy values were the same, within the experimental error, for both complexes (see Supplementary Material available online at doi: 10.4061/2010/763658). In addition, the CD spectra of both complexes in the presence of Mg^{2+}, Na^+, and Zn^{2+} were very similar to each other and to the B-form duplex (data not shown). In these conditions the G,T-parallel triplex was not formed. Instead parallel clamp **1** bounds its target, yielding the antiparallel Watson-Crick duplex.

3.2. 8-Aminoadenine and 8-Aminoguanine Stabilize G,T-Parallel Duplexes. Next, the effect of 8-aminoadenine in the G,T-parallel duplexes was studied in a different sequence. Three G,T-parallel duplexes were synthesized (4–7, Table 1) as described above using the phosphoramidite of 8-amino-2′-deoxyadenosine described elsewhere [20] and the phosphoramidite of 8-amino-2′-deoxyguanosine [21]. These oligonucleotides were designed to bind a well-studied, model polypyrimidine sequence (8, Table 1) [15, 21, 22]. Clamp **5** carries two 8-aminoadenine residues and clamp 6 carries four modifications. Clamp **7** carries two 8-aminoguanine residues.

The parallel duplex-to-random-coil transitions of duplexes **4–7** were measured at pH 7.2 in the presence of magnesium. As described above a single transition was observed which occurred at progressively higher temperatures as the number of 8-aminoadenine residues in the parallel-clamp increased (Table 2). When two adenines were replaced by two 8-aminoadenines, the melting temperature rose by 5.9°C (Table 2). This increase was 7°C when the number of adenine substitutions was four (Table 2). When two guanine residues were replaced by two 8-aminoguanines, the melting temperature rose by 5.5°C. This increase is similar to that produced by the presence of two 8-aminoadenines. The CD spectra of duplexes **4–6** consisted of a positive maximum at around 260 nm, zero-crossover at around 250 nm, and a negative band at around 240 nm (Figure 4). These spectra agree with previously

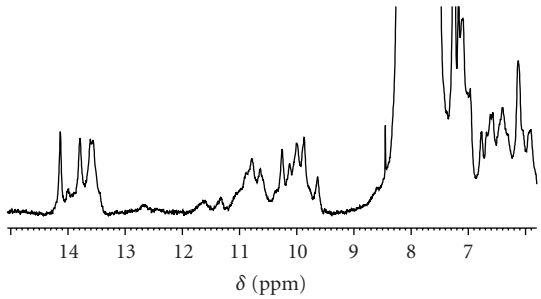

Figure 5: NMR spectrum of parallel duplex **7** (Conditions 50 mM $MgCl_2$, 10 mM sodium phosphate).

described CD spectra for G,T-parallel duplexes [24]. The intensity of the bands was proportional to the number of 8-aminoadenine residues (Figure 4). This is consistent with the more ordered duplex structure indicated by the increased *Tm* and free energy values obtained from UV-melting curves. A similar effect was observed for the intramolecular duplex carrying two 8-aminoguanine residues, **7**. The NMR spectrum of this duplex is shown in Figure 5. The sharp imino signals between 10 and 14 ppm are a clear indication of the presence of stable AT and GG base pairs. Contrary to the case of the unmodified duplex **1**, shown in Figure 3, duplex **7** forms a well-ordered and more compact parallel structure. We concluded that the presence of the 8-aminoadenine and 8-aminoguanine residues stabilizes G,T-parallel duplex.

3.3. Parallel Duplexes Carrying 8-Aminopurines Do Not Bind Their Polypyrimidine Targets. Next, the interaction of G,T-parallel duplexes with its polypyrimidine target **8** to form G,T-parallel triplexes was analyzed by UV, CD, and NMR spectroscopy as well as gel-shift analysis. The corresponding G,T-parallel triplex was not formed. When unmodified parallel-stranded duplexes were mixed with their polypyrimidine target, a Watson-Crick duplex was formed, leaving the G,T-strand unpaired as described above for oligonucleotides **1** and **2**.

Next we analyzed the melting curves of complexes formed by the parallel duplexes **4**–**7** and their polypyrimidine target **8** using UV-spectroscopy. A control antiparallel duplex was formed by mixing oligonucleotides **9** and **8**. Oligonucleotide **9** has the same polypurine sequence as parallel clamp **5** (with two 8-aminoadenine residues) linked to a scrambled G,T-sequence.

Complexes formed by parallel duplexes **4**–**7** and their polypyrimidine target **8** gave melting curves that were similar to those of the parallel duplexes **4**–**7** alone. Melting temperatures were practically indistinguishable from the *Tm* of the duplexes without targets (Supplementary, Table S2).

This pattern was clearly different from the duplex formed by mixing oligonucleotides **8** and **9**. No transition was observed when heating a solution of control oligonucleotide **9** alone. When mixed with the target sequence **8** a transition with a melting temperature at 44°C was observed. This melting temperature was lower than that of the complex formed by mixing **4** and **8** (55.6°C). This is in agreement with the decreased affinity of 8-aminoadenine for thymine in duplexes.

Complexes formed by parallel duplexes **4** and **5** as well as control oligonucleotide **9** with their 2′-O-methyl-RNA-polypyrimidine target **11** were also studied. As described above, melting curves of parallel duplexes with the target sequence were similar to those of the duplexes alone. Melting temperatures were practically indistinguishable from the *Tm* of the duplexes without targets (Supplementary, Table S2). However, in this case, the duplex formed by mixing control oligonucleotide **9** and target **11** gave a transition with a melting temperature at 50.4°C. This *Tm* is consistent with the higher stability of the RNA/DNA duplex versus DNA/DNA duplex. This increased *Tm* was not observed in the complexes formed by parallel duplexes.

The CD spectrum of the complex formed by mixing unmodified clamp **4** and its target **8** was different from that of the clamp alone. As described in Figure 2 for the complex between **1** and **2**, the negative band at 240 nm of the CD spectrum remained but the positive maximum moved to 277 nm and the zero-crossover moved to 255 nm (data not shown). This indicates that unmodified clamp **4** and its target **8** formed the antiparallel duplex. Surprisingly, the CD spectra of 8-aminoadenine duplexes **5** and **6** changed very little after mixing with their polypyrimidine target **8** (Supplementary Figure 1S). This indicates lack of interaction of 8-aminoadenine duplexes with their target. Gel-shift analysis confirms the lack of binding (see Supplementary Material).

In conclusion, parallel-stranded duplexes carrying 8-aminopurines did not bind to their target. The parallel-stranded duplex remained unaltered in the presence of the polypyrimidine target as judged by melting curves analysis, CD, and gel-shift analysis (see Supplementary Material).

3.4. Theoretical Analysis of the G,T-Parallel Duplexes. Theoretical simulations using state-of-the-art molecular dynamic techniques were used to gain structural details on the different duplexes/triplexes considered here and to rationalize the experimental results. Trajectories of parallel duplexes containing Hoogsteen d(A·T) and d(G·C^+) pairs (ps-Duplex I) are stable sampling structures whose helical characteristics are very close to those expected for a H-duplex [38], confirming our previous claims on the stability of H-duplex in mixed A-G sequences [15, 22, 39]. A completely different situation is found when the parallel duplex containing Hoogsteen-like d(A · T) and d(G · G) pairs is considered (ps-Duplex II), since the helical structure of this duplex is severely distorted in the 10-nanosecond time scale (Table 3 and Figure 6).

The distortion observed is localized not only at the ends, which tend to loose helicity (Figure 6), but also in the center of the helix, where severe transitions are found leading to a lost of nearly 50% of canonical Hoogsteen hydrogen bonds (Table 4). The most interesting of such transitions is a flip from Hoogsteen to reverse Watson-Crick pairings as expected in a rWC parallel duplex [38].

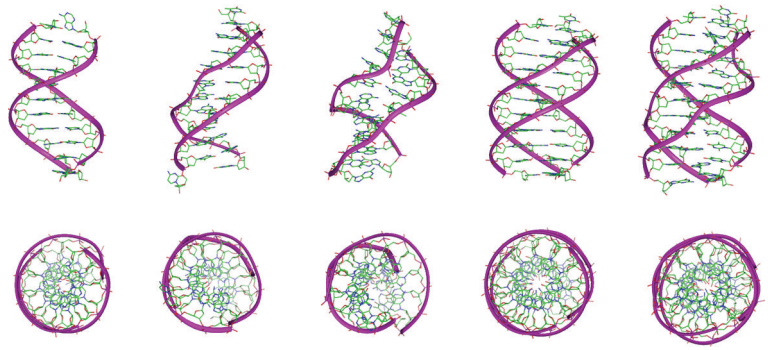

Figure 6: Representation of the average structures (obtained by relaxing Cartesian average in the 8th → 10th nanosecond) for the different duplexes and triplexes considered here.

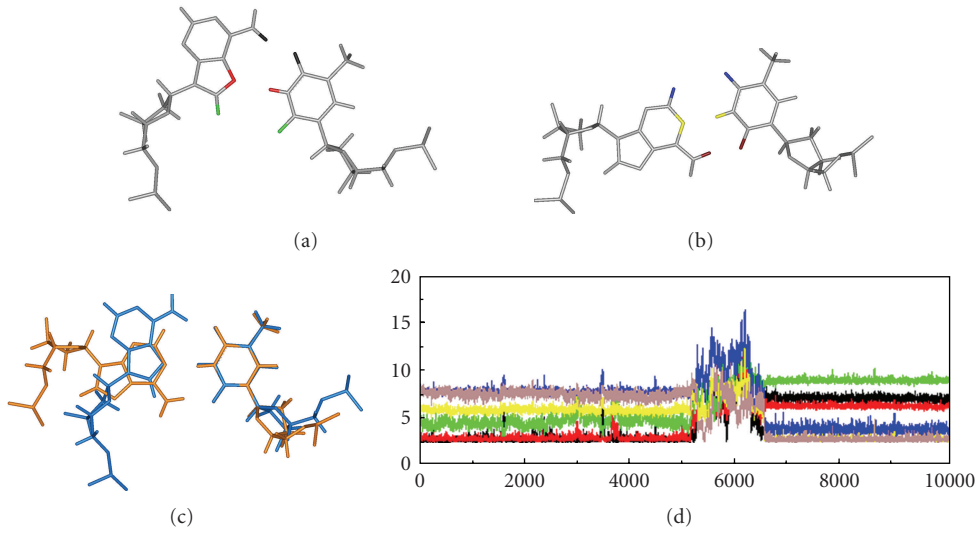

Figure 7: Representation of the geometry of d(A-T) pairs sampled during the MD simulation of ps-Duplex II. (a): Hoogsteen pair. (b): reverse-Watson-Crick. (c): superposition of both Hoogsteen and reverse-Watson Crick pairings. (d) detail of hydrogen bond distances in one of the pairs showing Hoogsteen → reverse Watson-Crick transitions. Color code: (i) Hoogsteen; Black: H6-O4; Red: N7-H3; Green: H8-O2; and (ii) reverse WC; Blue: H2-O4; Yellow: N1-H3; Light brown: H6-O2.

Table 3: Average root mean square deviation (RMSd in Å) between trajectories of the different duplexes and triplexes and the starting and average structures. The prefixes ps and aps refer to parallel and antiparallel topologies. Standard deviations in the averages are noticed in all cases.

	Sequence	Starting structure	Average structure
aps-Duplex	5′-AGAGGAGGAAG-3′ 3′-TCTCCTCCTTC-5′	2.5 ± 0.4	1.7 ± 0.3
ps-Duplex I	5′-AGAGGAGGAAG-3′ 5′-*TC$^+$ TC$^+$ C$^+$ TC$^+$ C$^+$ TTC$^+$*-3′	2.3 ± 0.5	2.2 ± 0.5
ps-Duplex II	5′-AGAGGAGGAAG-3′ 5′-*TGTGGTGGTTG*-3′	3.4 ± 0.7	2.8 ± 0.7
ps-Triplex I	5′-AGAGGAGGAAG-3′ 3′-TCTCCTCCTTC-5′ 5′-*TC$^+$ TC$^+$ C$^+$ TC$^+$ C$^+$ TTC$^+$*-3′	1.8 ± 0.3	1.2 ± 0.2
ps-Triplex II	5′-AGAGGAGGAAG-3′ 3′-TCTCCTCCTTC-5′ 5′-*TGTGGTGGTTG*-3′	1.9 ± 0.2	1.3 ± 0.3

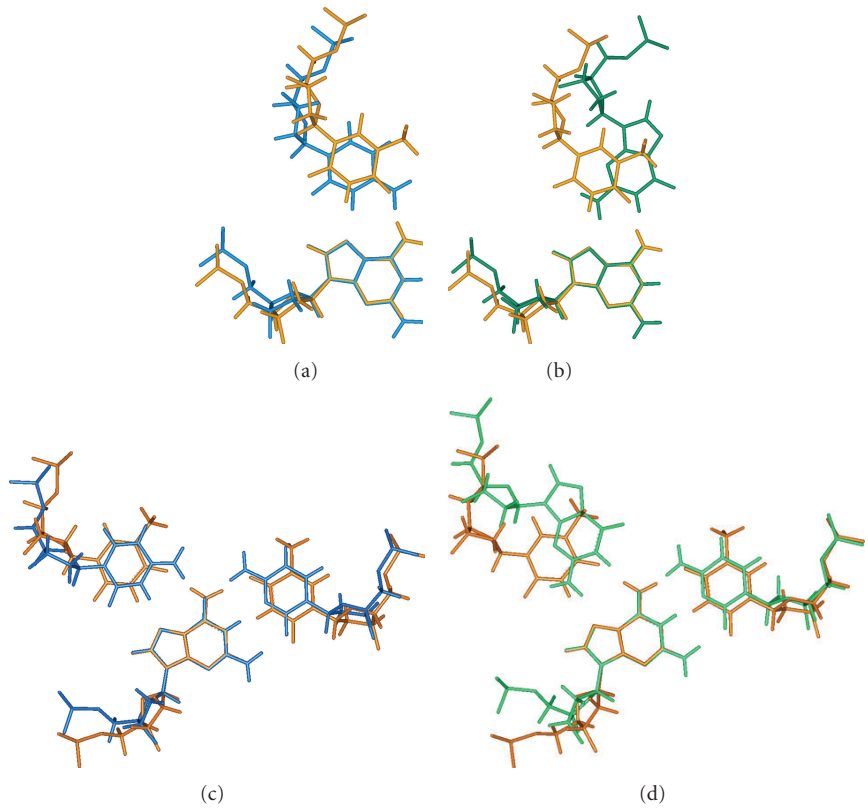

Figure 8: (a)-(b): Superposition of d(G-G) and d(G-C$^+$) pairs to the reference d(A-T) one in parallel DNA. (c)-(d): Superposition of d(G·C-G) and d(G·C-C$^+$) triads to the reference d(A·T-T) one in parallel triplex. In all the cases the central purine atoms were used as reference in the fitting.

Table 4: Percentage (from maximum number possible) of hydrogen bond detected in the different simulations. Partition between different types or pairs (A·T, A-T, G·C$^+$, and G-G) is included. [&]The total number of hydrogen bond includes reverse Watson-Crick hydrogen bonds detected in the trajectory.

	% HB Watson-Crick	% HB Hoogsteen	% HB Total
aps-Duplex	97.1 (93.1 A·T* & 99.4 G·C)	—	97.1
ps-Duplex I	—	85.7 (88.2 A-T & 83.5 G-C$^+$)	85.7
ps-Duplex II	—	52.9 (38.0 A-T & 65.4 G-G)	59.7[&]
ps-Triplex I	99.4 (98.6 A·T & 99.8 G·C)	90.9 (80.7 A-T & 99.4 G-C$^+$)	95.7
ps-Triplex II	96.3 (93.2 A·T* & 98.1 G·C)	73.5 (65.0 A-T & 80.6 G-G)	86.3

Analysis of the trajectories reveals that the lack of isomorphism in the Hoogsteen-like d(A-T) and d(G-G) pairs is mainly responsible for the instability of the parallel duplex (see Figure 7). Thus the different size of d(A-T) and d(G-G) pairs generates a large mechanical stress in the Hoogsteen backbone, resulting in either lost of helicity or disruption of the pattern of hydrogen bonds. Overall, it is clear that unrestricted MD simulations are very strongly suggesting that the parallel duplex with d(A · T) and d(G · G) pairs is not very stable and might exist not only as an H-duplex but also as a myriad of other helical or quasihelical conformations. MD simulations are then fully supporting the claims derived from the inspection of the CD and NMR spectra of these oligonucleotides (see above).

3.5. Theoretical Analysis of the G,T-Parallel Triplexes. As reported previously [26, 28], the parallel triplex (ps-Triplex I) with d(A·T-T) and d(G · C-C$^+$) triads is very stable, sampling B-like canonical triplex conformations [28], see Tables 3 and 4 and Figure 6. On the contrary, simulations of parallel triplexes containing d(A · T-T) and d(G · C-G) triads (ps-Triplex II) lead to distorted helical conformations in the 10-nanosecond time scale due to the disruptions in the structure of the Hoogsteen strand (see Tables 3 and 4 and Figure 5). Such distortions are reflected in anomalous backbone arrangements and in a significant lost of the expected Hoogsteen-like hydrogen bonds (Table 4). Clearly, the different geometry of d(A · T-T) and d(G · C-G) triads is the main reason for all these distortions which are expected to handicap the stability of the triplex (Figure 8).

Table 5: Cross RMSd (in Å) between trajectories and the average structures obtained in the other trajectories. When parallel duplexes and triplexes are compared only, the Hoogsteen duplex embedded in the triplex is considered.

	ps-Duplex		ps-Triplex (H)	
	Starting structure	Average structure	Starting structure	Average structure
ps-Duplex I	2.3 ± 0.5	2.2 ± 0.5	2.3 ± 0.5	2.1 ± 0.6
ps-Triplex I (H)	1.7 ± 0.2	2.2 ± 0.1	1.6 ± 0.2	1.1 ± 0.2
ps-Duplex II	3.4 ± 0.7	2.8 ± 0.7	3.3 ± 0.7	3.5 ± 0.8
ps-Triplex II (H)	2.0 ± 0.2	4.1 ± 0.3	2.0 ± 0.2	1.3 ± 0.3

Table 6: Free energy difference (in kcal/mol) in different folding processes associated to A → A^N mutation. A negative sign means that the presence of 8-aminoadenine stabilizes the folded form (right species in column 2).

Mutation	Folding process	$\Delta\Delta G_{stab\,(kcal/mol)}$
A → A^N	Single strand → ps-Duplex II	−2.8 ± 0.2
	Single strand → ps-Triplex II	−3.3 ± 0.2
	ps-Duplex II → ps-Triplex II	−0.5 ± 0.2

In previous works, we demonstrate both theoretically and experimentally that parallel stranded H-duplexes were perfectly preorganized to capture a pyrimidine Watson-Crick strand and generate a parallel triplex [15, 22]. This finding is confirmed here, since the cross-RMSd between the H-duplex (ps-Duplex I) and the Hoogsteen strands of the parallel triplex (ps-Triplex I) is small (Table 5). On the contrary, such a preorganization is lost for the ps-Duplex II, since this duplex displays an average conformation which is far from that required to form a parallel triplex (see Table 5).

Overall, all the theoretical results point into the same direction: ps duplexes with Hoogsteen-like d(A-T) and d(G-G) pairs display a reduced stability, a large structural irregularity, and an average conformation which is not ideal for triplex formation. Simulation results are then explaining apparently surprising experimental findings, demonstrating that despite that 2D representations might suggest that stable templates for triplex formation could be generated from suitable parallel hairpins with d(A-T) and d(G-G) pairings, the resulting structures are irregular and unstable and are poor templates for triplex formation.

3.6. The Effect of 8-Aminoadenine. As in previous studies [15, 20–23, 33, 40] MD/TI calculations were performed to evaluate the gain of stability of ps-Duplex II due to the change of one adenine (A) by one 8-aminoadenine (A^N). For this purpose one A → A^N mutation was performed for single stranded, duplex, and triplex and combined using the standard thermodynamic cycles (see *Methods* and references [15, 20–23, 33, 40]) to evaluate the impact of the mutation on the single-strand → ps-Duplex II, single-strand → ps-Triplex II, and ps-Duplex II → ps-Triplex II (see Methods) folding processes. Even if, as expected [15, 20–23, 30, 31], the presence of 8-aminoadenine does not introduce major structural changes, it largely stabilizes the ps- duplex (almost 3 kcal/mol from data in Table 6), in good agreement with the situation found for other parallel H-like duplexes [22] and with the melting experiments reported in this paper (see above). Not surprisingly, the presence of 8-aminoadenine theoretically stabilizes the parallel triplex as found in other cases [15, 20, 21, 32, 40]. However, the impact of the mutation in the ps-Duplex I → ps-Triplex I equilibrium is very small, suggesting that the presence of 8-aminoadenine stabilizes the H-duplex, but does not transform it into a more attractive template for the formation of triplex, in good agreement with our own experimental findings.

4. Conclusions

Present work completes the analysis of parallel stranded duplexes and their capability to act as templates for triplex formation upon interaction with a complementary polypyrimidine strand. Combination of accurate modelling techniques, synthetic chemistry, and biophysical techniques has allowed us to obtain a global picture of the nature of different hairpin-based parallel stranded duplexes, natural of 8-aminopurine substituted, and of their ability to act as templates for triplex formation with a target polypyridine strand. Results show that the isomorphism of the parallel helix is a crucial requirement for its stability and ability to act as template for triplex formation. Addition of 8-aminopurines can stabilize the H-duplex, which might have importance for the generation of aptamers, but it cannot transform the geometry of the helix, and accordingly modified duplex remains unable to form triplex. Results reported here suggest that parallel H-duplexes based on d(A-T) and d(G-C^+) duplexes, specially when purines are substituted by 8-amino derivatives, are the best templates for triplex generation based on capturing single DNA or RNA polypyrimidine strands.

Acknowledgments

This study was supported by the Dirección General de Investigación Científica y Técnica (Grants BFU2007-63287, BIO2006-01602, CTQ2007-68014-C02-02, Consolider Escience Project), the Generalitat de Catalunya (2005/SGR/00693), the Fundación Marcelino Botín, and the Fundació LA CAIXA (BM04-52-0).

References

[1] W. Saenger, in *Principles of Nucleic Acid Structure*, Springer, New York, NY, USA, 1994.

[2] V. N. Soyter and V. N. Potaman, in *Triple Helical Nucleic Acids*, Springer, New York, NY, USA, 1996.

[3] J.-S. Sun, T. Garestier, and C. Hélène, "Oligonucleotide directed triple helix formation," *Current Opinion in Structural Biology*, vol. 6, no. 3, pp. 327–333, 1996.

[4] J. R. Williamson, "G-quartet structures in telomeric DNA," *Annual Review of Biophysics and Biomolecular Structure*, vol. 23, pp. 703–730, 1994.

[5] K. Rippe and T. M. Jovin, "Parallel-stranded duplex DNA," *Methods in Enzymology*, vol. 211, pp. 199–220, 1992.

[6] J. H. van de Sande, N. B. Ramsing, M. W. Germann, et al., "Parallel stranded DNA," *Science*, vol. 241, no. 4865, pp. 551–557, 1988.

[7] P. V. Scaria and R. H. Shafer, "Calorimetric analysis of triple helices targeted to the $d(G_3A_4G_3)\cdot d(C_3T_4C_3)$ duplex," *Biochemistry*, vol. 35, no. 33, pp. 10985–10994, 1996.

[8] S. R. Bhaumik, K. V. R. Chary, G. Govil, K. Liu, and H. T. Miles, "NMR characterisation of a triple stranded complex formed by homo-purine and homo-pyrimidine DNA strands at 1:1 molar ratio and acidic pH," *Nucleic Acids Research*, vol. 23, no. 20, pp. 4116–4121, 1995.

[9] K. Liu, H. T. Miles, J. Frazier, and V. Sasisekharan, "A novel DNA duplex. A parallel-stranded DNA helix with Hoogsteen base pairing," *Biochemistry*, vol. 32, no. 44, pp. 11802–11809, 1993.

[10] E. J. Kremer, M. Pritchard, M. Lynch, et al., "Mapping of DNA instability at the fragile X to a trinucleotide repeat sequence p(CCG)n," *Science*, vol. 252, no. 5013, pp. 1711–1714, 1991.

[11] N. A. Tchurikov, A. K. Ebralidze, and G. P. Georgiev, "The suffix sequence is involved in processing the 3′-ends of different mRNAs in Drosophila melanogaster," *The EMBO Journal*, vol. 5, no. 9, pp. 2341–2347, 1986.

[12] N. A. Tchurikov, A. K. Shchyolkina, O. F. Borissova, and B.K. Chernov, "Southern molecular hybridization experiments with parallel complementary DNA probes," *FEBS Letters*, vol. 297, no. 3, pp. 233–236, 1992.

[13] R. Veitia and C. Ottolenghi, "Placing parallel stranded DNA in an evolutionary context," *Journal of Theoretical Biology*, vol. 206, no. 2, pp. 317–322, 2000.

[14] E. R. Kandimalla and S. Agrawal, "Hoogsteen DNA duplexes of 3′-3′- and 5′-5′-linked oligonucleotides and triplex formation with RNA and DNA pyrimidine single strands: experimental and molecular modeling studies," *Biochemistry*, vol. 35, no. 48, pp. 15332–15339, 1996.

[15] A. Aviñó, M. Frieden, J. C. Morales, et al., "Properties of triple helices formed by parallel-stranded hairpins containing 8-aminopurines," *Nucleic Acids Research*, vol. 30, no. 12, pp. 2609–2619, 2002.

[16] E. N. Brody and L. Gold, "Aptamers as therapeutic and diagnostic agents," *Reviews in Molecular Biotechnology*, vol. 74, no. 1, pp. 5–13, 2000.

[17] T. Mairal, V. C. Özalp, P. Lozano Sánchez, M. Mir, I. Katakis, and C. K. O'Sullivan, "Aptamers: molecular tools for analytical applications," *Analytical and Bioanalytical Chemistry*, vol. 390, no. 4, pp. 989–1007, 2008.

[18] N. T. Thuong and C. Hélène, "Sequence-specific recognition and modification of double-helical DNA by oligonucleotides," *Angewandte Chemie International Edition*, vol. 32, no. 5, pp. 666–690, 1993.

[19] P. P. Chan and P. M. Glazer, "Triplex DNA: fundamentals, advances, and potential applications for gene therapy," *Journal of Molecular Medicine*, vol. 75, no. 4, pp. 267–282, 1997.

[20] R. Güimil García, E. Ferrer, M. J. Macías, R. Eritja, and M. Orozco, "Theoretical calculations, synthesis and base pairing properties of oligonucleotides containing 8-amino-2′-deoxyadenosine," *Nucleic Acids Research*, vol. 27, no. 9, pp. 1991–1998, 1999.

[21] R. Soliva, R. Güimil García, J. R. Blas, et al., "DNA-triplex stabilizing properties of 8-aminoguanine," *Nucleic Acids Research*, vol. 28, no. 22, pp. 4531–4539, 2000.

[22] E. Cubero, A. Aviñó, B. G. de la Torre, et al., "Hoogsteen-based parallel-stranded duplexes of DNA. Effect of 8-amino-purine derivatives," *Journal of the American Chemical Society*, vol. 124, no. 12, pp. 3133–3142, 2002.

[23] A. Aviñó, E. Cubero, C. González, R. Eritja, and M. Orozco, "Antiparallel triple helices. Structural characteristics and stabilization by 8-amino derivatives," *Journal of the American Chemical Society*, vol. 125, no. 51, pp. 16127–16138, 2003.

[24] M. W. Germann, B. W. Kalisch, and J. H. van de Sande, "Structure of $d(GT)_n\cdot d(GT)_n$ sequences: formation of parallel stranded duplex DNA," *Biochemistry*, vol. 37, no. 37, pp. 12962–12970, 1998.

[25] E. B. Khomyakova, H. Gousset, J. Liquier, et al., "Parallel intramolecular DNA triple helix with G and T bases in the third strand stabilized by Zn^{2+} ions," *Nucleic Acids Research*, vol. 28, no. 18, pp. 3511–3516, 2000.

[26] R. Soliva, C. A. Laughton, F. J. Luque, and M. Orozco, "Molecular dynamics simulations in aqueous solution of triple helices containing $d(G\cdot C\cdot C)$ trios," *Journal of the American Chemical Society*, vol. 120, no. 44, pp. 11226–11233, 1998.

[27] E. Jiménez-García, A. Vaquero, M. L. Espinás, et al., "The GAGA factor of Drosophila binds triple-stranded DNA," *Journal of Biological Chemistry*, vol. 273, no. 38, pp. 24640–24648, 1998.

[28] G. C. Shields, C. A. Laughton, and M. Orozco, "Molecular dynamic simulations of the $d(T\cdot A\cdot T)$ triple helix," *Journal of the American Chemical Society*, vol. 119, no. 32, pp. 7463–7469, 1997.

[29] G. C. Shields, C. A. Laughton, and M. Orozco, "Molecular dynamics simulation of a PNA · DNA · PNA triple helix in aqueous solution," *Journal of the American Chemical Society*, vol. 120, no. 24, pp. 5895–5904, 1998.

[30] T. Darden, D. York, and L. Pedersen, "Particle mesh Ewald: an $N\cdot\log(N)$ method for Ewald sums in large systems," *The Journal of Chemical Physics*, vol. 98, no. 12, pp. 10089–10092, 1993.

[31] J.-P. Ryckaert, G. Ciccotti, and H. J. C. Berendsen, "Numerical integration of the cartesian equations of motion of a system with constraints: molecular dynamics of n-alkanes," *Journal of Computational Physics*, vol. 23, no. 3, pp. 327–341, 1977.

[32] E. Cubero, R. Güimil-García, F. J. Luque, R. Eritja, and M. Orozco, "The effect of amino groups on the stability of DNA duplexes and triplexes based on purines derived from inosine," *Nucleic Acids Research*, vol. 29, no. 12, pp. 2522–2534, 2001.

[33] A. Pérez, I. Marchán, D. Svozil, et al., "Refinement of the AMBER force field for nucleic acids: improving the description of α/γ conformers," *Biophysical Journal*, vol. 92, no. 11, pp. 3817–3829, 2007.

[34] W. D. Cornell, P. Cieplak, C. I. Bayly, et al., "A second generation force field for the simulation of proteins, nucleic acids, and organic molecules," *Journal of the American Chemical Society*, vol. 117, no. 19, pp. 5179–5197, 1995.

[35] T. E. Cheatham III, P. Cieplak, and P. A. Kollman, "A modified version of the Cornell et al. force field with improved sugar pucker phases and helical repeat," *Journal of Biomolecular Structure and Dynamics*, vol. 16, no. 4, pp. 845–862, 1999.

[36] W. L. Jorgensen, J. Chandrasekhar, J. D. Madura, R. W. Impey, and M. L. Klein, "Comparison of simple potential functions for simulating liquid water," *The Journal of Chemical Physics*, vol. 79, no. 2, pp. 926–935, 1983.

[37] D. A. Case, T. A. Darden, T. E. Cheatham III, et al., *AMBER 9*, University of California, San Francisco, Calif, USA, 2006.

[38] E. Cubero, F. J. Luque, and M. Orozco, "Theoretical studies of d(A:T)-based parallel-stranded DNA duplexes," *Journal of the American Chemical Society*, vol. 123, no. 48, pp. 12018–12025, 2001.

[39] A. Aviñó, J. C. Morales, M. Frieden, et al., "Parallel-stranded hairpins containing 8-aminopurines. Novel efficient probes for triple-helix formation," *Bioorganic and Medicinal Chemistry Letters*, vol. 11, no. 13, pp. 1761–1763, 2001.

[40] J. Robles, A. Grandas, E. Pedroso, F. J. Luque, R. Eritja, and M. Orozco, "Nucleic acid triple helices: stability effects of nucleobase modifications," *Current Organic Chemistry*, vol. 6, no. 14, pp. 1333–1368, 2002.